Journal of Neuroscience Research 87:1334–1342 (2009)

Low-intensity Treadmill Exercise-related Changes in the Rat Stellate Ganglion Neurons

**Renato Albuquerque de Oliveira Cavalcanti,[1] Demilto Yamaguchi da Pureza,[1] Mariana Pereira de Melo,[2] Romeu Rodrigues de Souza,[3] Cássia T. Bergamaschi,[4] Sandra Lia do Amaral,[5] Helen Tang,[6] Andrzej Loesch,[6] and Antonio Augusto Coppi Maciel Ribeiro[1]*

[1]Laboratory of Stochastic Stereology and Chemical Anatomy (LSSCA), Department of Surgery, College of Veterinary Medicine, University of São Paulo (USP), São Paulo, Brazil
[2]Department of Statistics, Institute of Mathematics and Statistics, University of São Paulo, Brazil
[3]Physical Education Postgraduate Course, São Judas Tadeu University, São Paulo, Brazil
[4]Department of Bioscience, Federal University of São Paulo, Santos, Brazil
[5]Department of Physical Education, Faculty of Science, UNESP–São Paulo State University, Bauru, Brazil
[6]Research Department of Inflammation, University College London Medical School, Royal Free Campus, London, United Kingdom

Stellate ganglion (SG) represents the main sympathetic input to the heart. This study aimed at investigating physical exercise–related changes in the quantitative aspects of SG neurons in treadmill-exercised Wistar rats. By applying state-of-the-art design-based stereology, the SG volume, total number of SG neurons, mean perikaryal volume of SG neurons, and the total volume of neurons in the whole SG have been examined. Arterial pressure and heart rate were also measured at the end of the exercise period. The present study showed that a low-intensity exercise training program caused a 12% decrease in the heart rate of trained rats. In contrast, there were no effects on systolic pressure, diastolic pressure, or mean arterial pressure. As to quantitative changes related to physical exercise, the main findings were a 21% increase in the fractional volume occupied by neurons in the SG, and an 83% increase in the mean perikaryal volume of SG neurons in treadmill-trained rats, which shows a remarkable neuron hypertrophy. It seems reasonable to infer that neuron hypertrophy may have been the result of a functional overload imposed on the SG neurons by initial posttraining sympathetic activation. From the novel stereological data we provide, further investigations are needed to shed light on the mechanistic aspect of neuron hypertrophy: what role does neuron hypertrophy play? Could neuron hypertrophy be assigned to the functional overload induced by physical exercise?

Key words: stereology; extrinsic cardiac innervation; physical exercise; stellate ganglion; rats

The stellate ganglion (SG) is the main extrinsic innervation supplier to the heart (Wallis et al., 1996; Krout et al., 2003). The interruption of sympathetic pathways leading toward a particular region of the left ventricle induces asynchronous myocardial contraction, with putative adverse effects in left ventricular function (Skarda et al., 1986). In contrast, long-term benefits of SG blockade have been reported in human patients with severe chronic refractory angina (Chester et al., 2000). In hypertensive (but not hyperactive) rats, SG neurons undergo hypertrophy and an increase in dendritic length and number (Peruzzi et al., 1991).

Several studies have reported on the relation between stellate ganglia and physical exercise via pharmacological or hemodynamic approaches. For example, stellectomy was shown to lead to dysrhythmias consisting of supraventricular, atrioventricular junctional, or ventricular tachycardias after dogs are submitted to strenuous exercise in a treadmill (Randall et al., 1976). Conversely, infrastellate upper thoracic sympathectomy results in relative bradycardia during exercise, irrespective of which side was operated on, although clinical tolerance seems excellent in endurance exercise (Abraham et al., 2001). Along the same lines, significant peripheral presynaptic components (including nitric oxide) reducing the posttraining heart rate (HR) response to sympathetic activa-

Contract grant sponsor: FAPESP (Fundação de Amparo à Pesquisa do Estado de São Paulo); Contract grant number: 05/02411-1.

*Correspondence to: Antonio Augusto Coppi Maciel Ribeiro, Departamento de Cirurgia, Faculdade de Medicina Veterinária e Zootecnia, Universidade de São Paulo, Av. Prof. Dr. Orlando Marques de Paiva, 87-CEP 05508-270, São Paulo-SP, Brazil. E-mail: guto@usp.br

Received 26 May 2008; Revised 3 October 2008; Accepted 6 October 2008

Published online 29 December 2008 in Wiley InterScience (www.interscience.wiley.com). DOI: 10.1002/jnr.21961

tion have been reported (Mohan et al., 2000). In addition, unilateral stellate blockade in humans does not induce untoward cardiovascular effects during rest or exercise (Gardner et al., 1993).

However, to our knowledge, there are no morphoquantitative studies that use either biased or unbiased counting methods to investigate SG responses to physical exercise. Therefore, this study sought to investigate, by unbiased counting methods, the structural adaptations of the SG induced by low-intensity physical training. The research is also relevant to applied sports medicine and physiology of exercise.

MATERIALS AND METHODS

Animals and Materials

Ten left SGs from male Wistar rats were obtained from the College of Veterinary Medicine Animal Facility of the University of São Paulo, São Paulo, Brazil. Animals were divided into two groups ($n = 5$). Group I comprised untrained rats (140 days old, mean initial body weight 389 g), and group II comprised trained rats (140 days old, mean initial body weight 391 g). The study was approved by the Animal Care Committee of the College of Veterinary Medicine of the University of São Paulo (application 05-02711).

Low-intensity Physical Exercise

Adaptation phase. Rats were assigned to numbers, and we used an ordinary statistical table to systematically, uniformly, and randomly choose animals by means of a fixed fraction (Fn: 2^{-1}) of those numbers, e.g., animals 1, 3, 5, 7, and 9 formed group I, and animals 2, 4, 6, 8, and 10 formed group II. Group numbers—I or II—were chosen in the same way. Subsequently, rats were adapted to running on a motorized Inbramed treadmill for 10 min a day (at a 0.3 $km \cdot hr^{-1}$ speed) during 5 days before beginning the proper training (American College of Sports Medicine, 2006). An important criterion when ultimately selecting the animals was their ability to walk and run on the treadmill track.

Maximal graded treadmill exercise test. After a 5-day adaptation period, animals were subjected to a treadmill exercise test (TET-1) to achieve their maximal effort and determine the optimal training intensity. Animals were also tested in weeks 5 (TET-2) and 10 (TET-3) after the training program had commenced. Untrained rats were tested at the same time points. The initial test speed was 0.3 $km \cdot hr^{-1}$, and this was followed by progressive increments of 0.3 $km \cdot hr^{-1}$ every 3 min, until the animal was exhausted. The maximal training intensity was determined because rats were unable to run voluntarily after strenuous exercise (Silva et al., 1997).

Training program. After the maximal treadmill exercise test, animals were accordingly submitted to the training program on a motorized Inbramed treadmill. The duration, mean speed, and stage of the training sessions were, respectively, 30 min; 0.3 $km \cdot hr^{-1}$; week 1; 30 min; 0.5 $km \cdot hr^{-1}$; weeks 2 and 3; 30 min; 0.6 $km \cdot hr^{-1}$; week 4; 30 min; 0.7 $km \cdot hr^{-1}$; week 5; 30 min; 0.8 $km \cdot hr^{-1}$; week 6; 30 min; 0.9 $km \cdot hr^{-1}$; weeks 7 and 8; 30 min; 1.0 $km \cdot hr^{-1}$; weeks 9 and 10. Animals trained twice a day and worked out at 65% of the maximal training intensity. Each session lasted 30 min, and between these two sessions, there was a 4-hr interval. During the training program, untrained animals ran onto a treadmill for 5 min once a week at 0.4 $km \cdot hr^{-1}$ speed to keep them adapted to the machine (De Angelis et al., 2000). The training program efficiency was calculated as the speed increment between two consecutive maximal graded TETs (Silva et al., 1997).

Hemodynamic Parameters

In animals from groups I and II, after the last training session, two catheters filled with 0.06 ml of a saline solution were implanted under halothane anesthesia. Subsequently, the femoral artery and vein (PE-10) were cannulated for direct measurements of systolic pressure (SAP), diastolic pressure (DAP), and mean arterial pressure (MAP). Rats receiving food and water ad libitum were studied 1 day after catheter placement. All animals were conscious and unrestrained—that is, they were allowed to move freely during experiments. The arterial cannula was connected to a strain gauge transducer (P23Db, Gould-Statham, Oxnard, CA), and blood pressure (BP) signals were recorded over a 20-min period by a microcomputer equipped with an analog-to-digital converter board (CODAS, 1-kHz sampling frequency, Dataq Instruments, Akron, OH). The recorded data were analyzed on a beat-to-beat basis at a frequency of 100 Hz. The HR was obtained from arterial BP pulses.

Histology

Animals were sedated with azaperone (2 mg/kg, i.m.) followed by atropine sulphate (0.06 mg/kg, i.m.). For the anesthesia, a combination of ketamine chloride (10 mg/kg, i.m.) and xylazine hydrochloride (1.5 mg/kg, i.m.) (Bayer) was used, and the euthanasia procedure was conducted by administering an overdose of sodium pentobarbital (100 mg/kg, i.p.).

A bulbed cannula was inserted into the left ventricle and a cleaning solution of phosphate-buffered saline (Sigma; 0.1 M; pH 7.4) containing 2% heparin (Roche), and 0.1% sodium nitrite (Sigma) was injected into the ascending aorta and followed by a perfusion–fixation with a modified Karnovsky solution (5% glutaraldehyde and 1% formaldehyde) in a sodium cacodylate buffer (EMS; 0.125 M; pH 7.4). Left SGs were then dissected out, weighed, and their wet weights converted into volumes, assuming a tissue density of 1.06 $g \cdot cm^{-3}$, in order to estimate tissue deformation (shrinkage) (Brüel and Nyengaard, 2005). In addition, SG thickness, width, and length were measured with a digital pachymeter (Digimess).

In order to produce isotropic and uniform random sections, left SGs were embedded in i-sectors filled with 7% agar (Nyengaard and Gundersen, 1992). By means of a tissue slider, SGs were systematically, uniformly, and randomly cut into 1.0-mm-thick slabs, generating seven slabs in untrained and trained rats. Each slab was halved, producing on average 14 tissue blocks in untrained and trained rats. Subsequently slabs were washed in a sodium cacodylate buffer, postfixed in a solution of 2% osmium tetroxide in a sodium cacodylate buffer, stained en bloc with an aqueous solution saturated with uranyl

acetate (EMS), dehydrated in graded ethanol concentrations and propylene oxide (EMS), and embedded in Araldite 502 EMS. Specimens were polymerized in the oven at 60–70°C for 3 days. For light microscopy, 0.5- and 1-μm-thick sections were then cut with glass knives, collected onto glass slides, dried on a hot plate, stained with an 1% alcoholic toluidine blue solution, and mounted under a coverslip with a drop of Araldite. Section images were acquired with a Leica DMR microscope equipped with a DFC 300 FX Leica Digital Camera and projected onto a computer monitor.

Stereology (Design-based)

A modification of the physical disector method (Gundersen, 1986) was performed in this present study and comprised a reference and two lookup sections, and therefore two disector heights. This procedure was adopted to estimate neuronal numerical density and, finally, to estimate the mean neuronal volume (see SG mean neuron volume estimate).

Numerical density of SG neurons: N_V(neurons, SG). The method consists in counting the number of neurons that are present in unbiased counting frames on reference sections, which touch neither the forbidden lines of the frames nor their extensions, and which disappear in parallel lookup sections. The formula for the N_V estimation is $N_V = \sum Q^-(\text{SG cell})/\sum V(\text{SG})$ where $\sum Q^-$ represents the cell count and $\sum V(\text{SG})$ is the volume of all disectors sampled. The latter is estimated as $\sum P \cdot (a:p) \cdot h$, where P is the number of test points, (a:p) the area associated with each test point, and h the distance between disector planes (disector height).

Unbiased counting frames (area = 55,633 μm^2) (Gundersen, 1977) were systematically, uniformly and randomly superimposed onto section fields of view, and the same sampled area was followed toward eight consecutive sections, i.e., one 1-μm-thick section followed by another 0.5-μm-thick section and six more 1-μm-thick sections. The two disector heights used were 0.5 μm for nucleolus sampling and 7.5 μm for cell body sampling. Disectors were SUR applied in all SG slabs (Gundersen et al., 1999). On average, 47 disectors were used to count 150 cells in untrained and 49 disectors to count 154 cells in trained rats. The mean number of disectors applied per SG slab was 6 and 7 in untrained and trained rats, respectively.

Volume of ganglion: V(SG). The total volume of SG was estimated by means of the Cavalieri principle. Briefly, SG Araldite-embedded blocks were exhaustively and serially sectioned, and every 300th section (K = 300) was sampled and measured for cross-sectional area. The volume estimation was performed in a fraction (Fn = 2^{-1}) of the reference sections used for disectors. Then $V(SG) = \sum P \cdot (a:p) \cdot K \cdot BA$, where P is the number of test points hitting the reference space (P = 300), (a:p) the area associated with each test point (a:p = 98,758 μm^2), and BA is the block advance (BA = 0.5–1 μm). The error variance of the Cavalieri estimate (CE) was estimated according to Gundersen et al. (1999) and Nyengaard (1999). The CE was 0.06 for untrained and 0.05 for trained rats.

Shrinkage volume (%) was estimated to be (mean ± SD) 5.56 ± 1.51 in untrained and 7.27 ± 1.11 in trained rats. No correction for global shrinkage was made because differences between groups were not significant.

Total number of SG neurons: N (neurons, SG). The total number of SG neurons was estimated by multiplying N_V by SG volume: $N = [N_V \cdot V(SG)]$. The error variance of total number of neurons (CE(N)) was estimated as shown in Gundersen et al. (1999) and Nyengaard (1999). CE(N) was 0.09 and 0.07 for untrained and trained rats, respectively.

Volume density of SG neurons: V_V (neurons, SG). The fractional volume of SG occupied by SG neurons was determined by point counting in the same sections and using the same number of points used for the CE. A SUR sample of fields was yielded and test points were randomly superimposed on a computer monitor. The total number of points falling within the SG $\sum P(\text{ref})$ and the total number of points falling on neurons ($\sum P(\text{SG})$ neurons) were counted. Volume density was therefore estimated as

$$V_V = \sum P(\text{SG})\,\text{neurons} / \sum P(\text{ref}).$$

The error variance (CE) for the volume fractions (V_V) was estimated according to Nyengaard (1999) and was 0.05 for untrained and 0.04 for trained rats.

Total volume of SG neurons: V(neurons, SG). The total volume of SG neurons was indirectly estimated by multiplying their respective fractional volumes by the total volume of SG, V(SG) (Lima et al., 2007).

Mean volume of SG neurons: $\bar{v}_N$ (neurons, SG). The mean perikaryal volume of SG neurons was estimated by the Nucleator method (Gundersen, 1988) in the reference sections used for neuron total number estimation. Cells were unbiased selected by means of a second disector of height 0.5 μm. On average, 110 nerve cells were measured in untrained and 117 nerve cells were measured in trained rats. The following formula was used to estimate the neuron size:

$$\bar{v}_N = \sum (4\pi/3) \cdot \bar{l}_n^3$$

where $\bar{l}_n^3$ is the mean cubed distance from a cell central point (nucleolus) to cell boundaries.

Statistical Analysis

Normally distributed data were tested by *t*-test and one-way analysis of variance by Minitab version 15 software (2007). Normal distribution was ensured by the Anderson-Darling test, and equality of variances was tested by Levene's test. Results are shown as mean observed coefficient of variation (CV_{obs}), where CV_{obs} = SD/mean.

RESULTS

Body weight was reduced in trained (400 g) (0.14) when compared with untrained rats (493 g) (0.13). Intergroup differences reached statistical significance ($P = 0.03$).

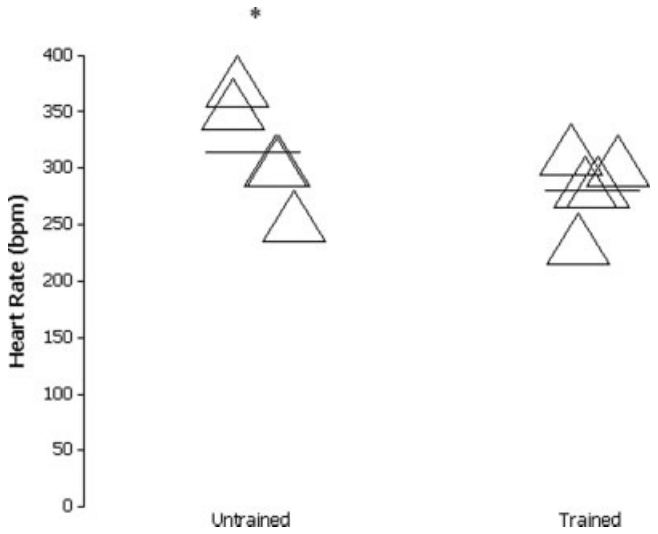

Fig. 1. HR in untrained and trained rats. Intergroup differences were significant (*$P = 0.02$). Triangles indicate individual values within a group; horizontal bars show group means.

Training Program

The training program efficiency was 133% between weeks 1 (0.3 km·hr^{-1}) (TET-1) and 5 (0.7 km·hr^{-1}), and 42% between weeks 5 (TET-2) (0.7 km·hr^{-1}) and 10 (TET-3) (1.0 km·hr^{-1}). Differences in training program efficiency were significant between TET-1 and TET-2 ($P = 0.0001$), and between TET-2 and TET-3 ($P = 0.01$).

Hemodynamic Parameters

In untrained rats, SAP, DAP, MAP, and HR were 132 mm Hg (0.14), 95 mm Hg (0.17), 107 mm Hg (0.18) and 314 bpm (0.20), respectively. In trained rats, SAP, DAP, MAP, and HR were 130 mm Hg (0.17), 94 mm Hg (0.15), 106 mm Hg (0.11) and 280 bpm (0.21), respectively. Intergroup differences were exclusively significant for HR ($P = 0.02$) (Fig. 1).

Anatomy

In all animals, irrespective of physical exercise, left SGs were irregularly shaped and located at the level of the first and second thoracic vertebrae. Dorsally, ganglia were in contact with the bodies of first and second thoracic vertebrae, and their caudal pole continued into the thoracic sympathetic trunk.

In untrained rats, SG length, width, and thickness were 7.08 mm (0.17), 1.26 mm (0.23), and 0.81 mm (0.17), respectively. In trained rats, the values were 7.82 mm (0.24), 1.14 mm (0.25), and 0.83 mm (0.17), respectively. Differences between groups did not attain statistical significance for ganglion length ($P = 0.124$), width ($P = 0.217$), and thickness ($P = 0.869$).

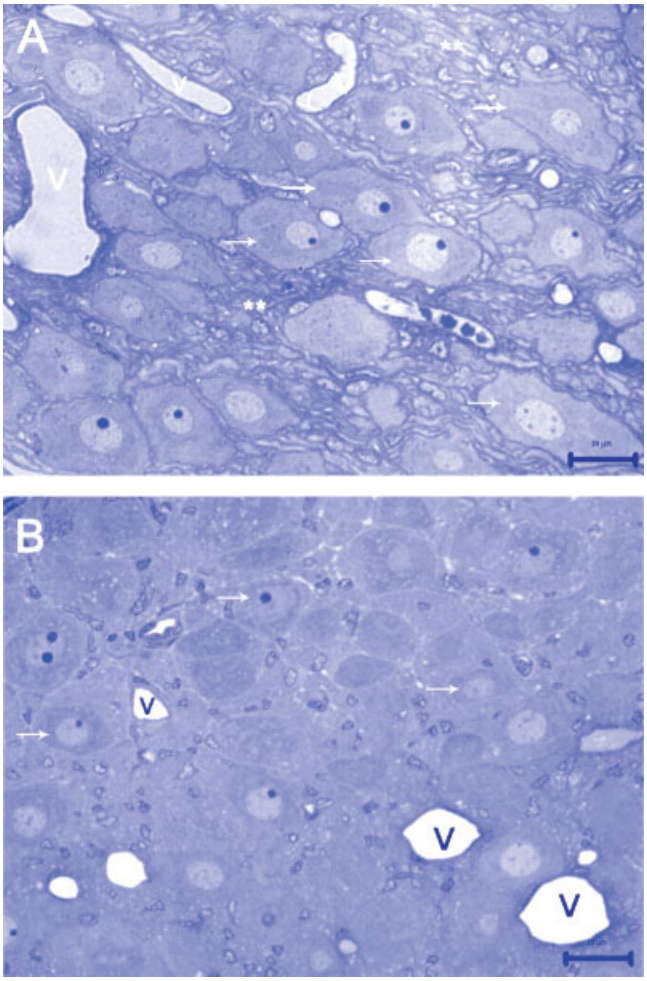

Fig. 2. Structure of the SG of a trained (**A**) and untrained rat (**B**) in semithin sections (0.5 μm) at the same magnification. In trained rats, larger nerve cell bodies (arrows) are further apart because they are separated by large spaces mainly occupied by nonneuronal tissue (**) and vessels (V). SG neurons from untrained rats were smaller (arrows), irregularly clustered, and separated by vessels (V). Toluidine blue. Scale bar = 20 μm. [Color figure can be viewed in the online issue, which is available at www.interscience.wiley.com.]

Histology

In semithin sections, left SGs consisted of clusters of neurons separated by nerve fibers, blood vessels, and prominent septa of connective tissue, mainly in trained rats. Ganglion neuron profiles were circular or, more commonly, oval shaped (Fig. 2). SG neurons were more irregularly clustered in untrained (Fig. 2B) than in trained rats (Fig. 2A). In all groups, most of the nuclei were located in the center of the perikaryon while a minority was eccentric, but none was located at the periphery of the neuronal profiles (Fig. 2).

Volume of ganglion: V(SG). The SG volume was 0.49 mm^3 (0.07) in untrained and 0.47 mm^3 (0.15) in trained rats. Intergroup differences were not significant ($P = 0.648$) (Fig. 3).

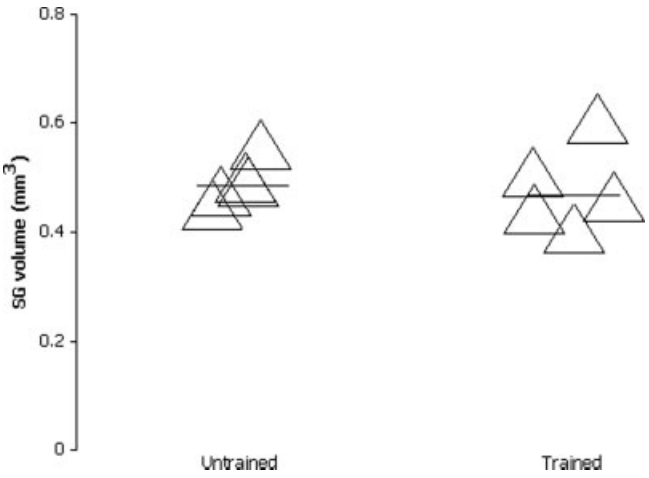

Fig. 3. SG volume in untrained and trained rats. There were no significant differences between groups ($P = 0.648$). Triangles indicate individual values within a group; horizontal bars show group means.

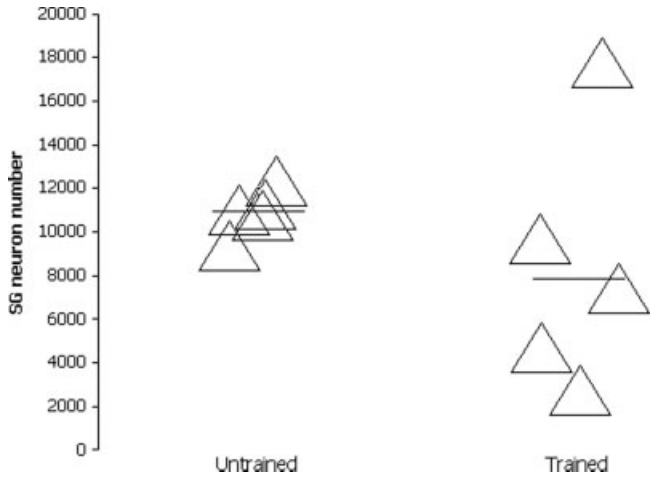

Fig. 4. Total number of neurons in the SG of untrained and trained rats. Intergroup differences were not significant ($P = 0.245$). Triangles indicate individual values within a group; horizontal bars show group means.

Numerical density of SG neurons: N_V (neurons, SG). The numerical density of SG neurons was 22,422 mm^{-3} (0.05) in untrained and 20,452 mm^{-3} (0.25) in trained rats. Nonsignificant differences were noted between groups ($P = 0.429$).

Total number of SG neurons: N (neurons, SG). The total number of SG neurons was 10,954 (0.06) in untrained and 7,841 (0.70) in trained rats. Differences between groups were not significant ($P = 0.245$) (Fig. 4).

Volume density of SG neurons: V_V (neurons, SG). The volume density of SG neurons was 0.47 (0.09) in untrained and 0.57 (0.07) in trained rats. Differences between groups attained statistical significance ($P = 0.009$).

Total volume of SG neurons: V (neurons, SG). The total volume occupied by SG neurons in the SGs was 0.23 mm^3 (0.18) in untrained and 0.27 mm^3 (0.15) in trained rats. Intergroup differences were not significant ($P = 0.201$) (Fig. 5).

Mean volume of SG neurons: $\bar{v}_N$ (neurons, SG). The mean perikaryal volume of SG neurons was 9,749 μm^3 (0.53) in untrained and 17,881 μm^3 (0.18) in trained rats. Intergroup differences were significant ($P = 0.017$) (Figs. 6 and 7).

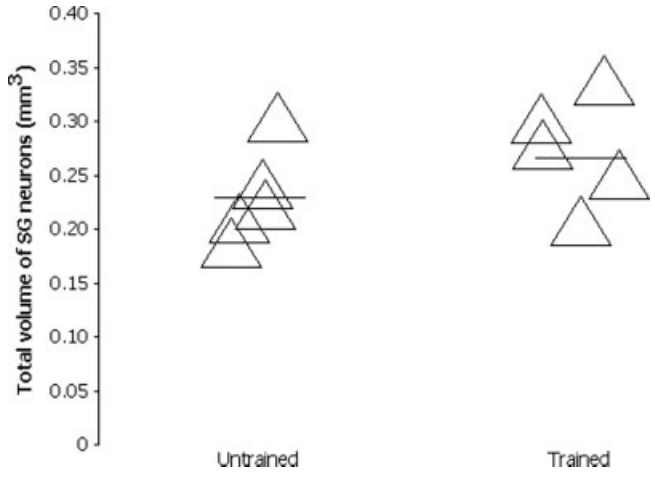

Fig. 5. Total volume of neurons in the SG of untrained and trained rats. Intergroup differences did not attain statistical significance ($P = 0.201$). Triangles indicate individual values within a group; horizontal bars show group means.

DISCUSSION

Methodological Approach for Quantification

Autonomic ganglia of the size of SG need to be sectioned to estimate cell size and number. By means of design-based stereological methods, counts and measurements may be performed onto a fraction of sections, rather than on the entire set of sections that the ganglion could generate. In order to achieve this, we have used disectors that are at the moment the most accurate (Sterio, 1984; Mayhew and Gundersen, 1996). For this study, three-dimensional quantitative microscopy was carried out onto histological preparations, which were as much as possible protected from artefacts, and which allowed for confidence in both cell identification and measurements. In addition, stereological estimations provide us with coefficient of errors for each estimate, which indicate the precision of the counting methods (Gundersen et al., 1999). Three technical improvements were important to this achievement: 1) vascular perfusion fixation, a procedure that delivers the fixative quickly and close to every cell, and prevents the collapse of the vascular space; 2) Araldite embedding rather than paraffin embedding, which, although some tissue deformation is unavoidable, minimizes other distortions, thermal damage, and cracking of the tissue; and 3) semithin sections were cut with glass knives at 0.5 and 1 μm

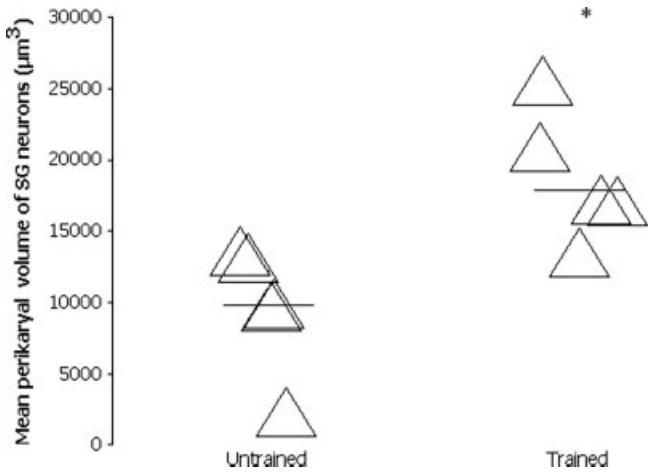

Fig. 6. Mean perikaryal volume of neurons in the SG of untrained and trained rats. Intergroup differences were significant (*P = 0.017). Triangles indicate individual values within a group; horizontal bars show group means.

thickness, generating sharp cell outlines that were easily identified, counted, and measured.

Hemodynamic Parameters

The present study demonstrates that a low-intensity exercise training program caused a 12% decrease in the HR of trained rats. This finding is in line with recent literature, though the findings are still mechanistically unclear and paradoxical. Early studies have shown that HR is the main determinant of the duration of left ventricle ejection systole in bicycle ergometer-trained young and middle-aged healthy men, although stroke volume and aortic BP exert secondary effects (Foster, 1956; Jones and Foster, 1964). However, bicycle ergometer-trained angina pectoris middle-aged men had decreases of cardiac output, stroke volume, and mean rate of ventricular ejection at any given HR (Foster and Reeves, 1964).

One possible source of bradycardia may be the post-training increase in the potassium transmembrane gradient in pacemaker cells, which increases extracellular potassium concentration in the myocardium decreasing its contractile properties (Negrão et al., 1992; Brum et al., 2000). Another possibility might be the presence of significant peripheral presynaptic components (including nitric oxide) in the stellate ganglia reducing the HR response to sympathetic activation after training (Mohan et al., 2000). However, it has recently been postulated that the resting bradycardia induced by regular physical exercise is due to an exacerbation of parasympathetic activity associated with decrements of the sympathetic input to the heart (Freeman et al., 2006). Along similar lines, other studies have suggested that exercise training may reduce sympathoexcitation by diminishing the activation of specific neurons within cardiovascular regions of the brain (Mueller, 2007) or by reducing the

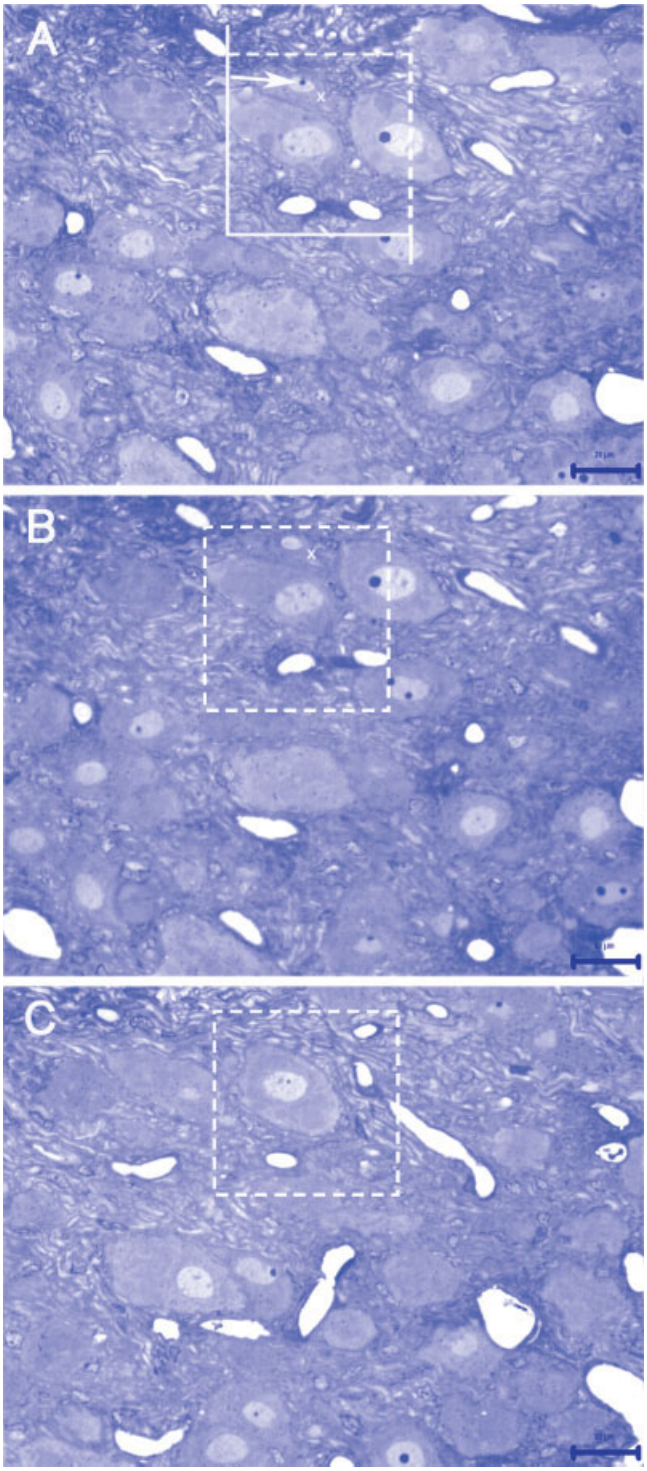

Fig. 7. Example of a disector-sampled SG neuron (*) used for neuronal volume (nucleator method) and number estimations. The reference (A) and lookup 1 sections (B) are separated by a height of 0.5 µm, and reference (A) and lookup 2 sections (C) are separated by a height of 7.5 µm. **A:** Neuronal cell body profile (*) that is no longer present in the lookup 2 section (**C**); arrow points a nucleolus profile that disappears in lookup 1 section (**B**) and was therefore sampled for neuron volume estimation. Toluidine blue. Scale bar = 20 µm. [Color figure can be viewed in the online issue, which is available at www.interscience.wiley.com.]

density or affinity of β adrenoceptors for cardiac tissue and as a result diminishing the chronotropic response to exercise (Nieto et al., 1996). Because our study is primarily focused on the quantitative morphology of SG, we cannot conclusively explain the postexercise bradycardia. In our experiment, we have not performed selective pharmacological analyses of the autonomic nervous control of HR so cannot shed light on this issue.

Another hemodynamic parameter measured in our study was the BP, and although our training program led to decreases of 1.54%, 1.06%, and 0.94% in SAP, DAP, and MAP, respectively, values did not reach statistical significance. Different from our results, low- to moderate-intensity exercise training seems to be a potential nonpharmacological strategy for the control of mild and borderline hypertension. However, the mechanisms involved in the attenuation of hypertension in such conditions are still controversial and not fully understood (Somers et al., 1991; Silva et al., 1997). On the other hand, it is known that physical training reduces the arterial pressure in hypertensive animals, although this may have no effects on the arterial pressure of normotensive trained animals (Amaral et al., 2000; O'Sullivan and Bell, 2000).

Reduction in peripheral resistance, sympathetic nerve activity, plasma levels of norepinephrine, and cardiac output have been associated with a decrease in BP (Kokkinos and Papademetriou, 2000). However, there is still controversy over the effects of training in normotensive subjects. Early studies that used physical exercise to reduce BP had paradoxical results, with some reporting reduction, increase, or no effect on BP (Cox, 2006). The latter was also found in our work. Again, although a mechanistic BP assessment was not the aim of this study, we agree with Cox (2006), who reported that these different and discrepant BP findings may be due to different effects attributed to several aerobic training programs used by previous studies, i.e., walking, swimming, cycling, treadmill, and voluntary wheel running. In addition, BP reduction during exercise can be also based on a decrease in systemic vascular resistance, in which the sympathetic nervous system, the renin–angiotensin system, and decreases of plasma norepinephrine appear to be involved, irrespective of HR reduction (Cornelissen and Fagard, 2005). Indeed, a recent study has shown a 10% reduction in the BP of treadmill-trained spontaneously hypertensive rats that was accompanied by no changes in the HR. The BP reduction was actually attributed to changes in the wall-to-lumen ratio in muscle arterioles (Amaral et al., 2000).

Stereology

Myocardial structural changes induced by chronic exercise were the subject of both qualitative and morphoquantitative studies. By means of planimetry, Bozner and Meessen (1969) showed an increase in myocyte mitochondrial mass and in the mitochondria-to-myofibril ratio in the rat hearts as a result of swimming exercises. For instance, a recent study published by Eisele et al. (2008) described quantitative structural changes in the volume and number of cardiomyocytes and their mitochondria content in the left heart ventricle of mice after voluntary wheel running. The left ventricle of trained mice had 1.87-fold more mitochondria, and they were 1.26-fold smaller in volume. However, our study describes, for the first time, quantitative and structural adaptations of SG neurons that result from a low-intensity treadmill exercise program. Along the same lines, this is the first study that addresses the above question by means of state-of-the-art design-based stereology, which provides researchers with a battery of methodological estimation tools and their coefficients of error, allowing for robust and accurate conclusions (Gundersen et al., 1999).

We have therefore shown that the physical exercise program used in this experiment did not exert any influence on either ganglion size or total number of neurons. By the same token, the number of cardiomyocytes is not altered by voluntary wheel running (Eisele et al., 2008). Another treadmill-related finding was the 21% increase in the fractional volume occupied by neurons in the stellate ganglia of trained rats. However, volume density (or volume fraction) itself is not conclusive, and most conclusions that are based on ratios are misleading. This problem is addressed by design-based stereology and is called ''reference trap''—i.e., the lack of knowledge of the reference volume (Braendgaard and Gundersen, 1986; Mayhew, 2008). In our study, the reference volume—the SG volume—was known.

From the structural point of view, the most important outcome of this study was the 83% increase in the mean perikaryal volume of neurons in stellate ganglia of treadmill-trained rats. This remarkable neuron hypertrophy explains why neuron fractional volume increases, i.e., neurons get bigger and occupy a larger fraction of SG. However, SG as a whole does not change in size. The possibility cannot be excluded that this is due to the decrease in size and/or compression of other ganglion components such as nerve fibers or nonneuronal cells and tissues, e.g., fibroblasts, glial cells, mast cells, blood vessels, and extracellular matrix of connective tissue (Ribeiro et al., 2004; Ribeiro, 2006). At the time of writing, the challenging aspect is to explain why neurons from SG do hypertrophy. It seems reasonable to hypothesize that neuron hypertrophy is a structural response to the functional overload imposed by physical exercise and a response to the sympathetic activation or recruitment, which normally occurs after training (Mohan et al., 2000). As a result, significant peripheral presynaptic components (including nitric oxide) in the stellate ganglia would be recruited, reducing the positive chronotropic response to sympathetic nerve stimulation, and would therefore attenuate the postexercise HR response (Mohan et al., 2000). In the central nervous system, neuron hypertrophy has also been reported as a mechanism to compensate for neuronal loss during aging or functional overload (Cabello et al., 2002).

Conclusions and Remarks for Further Studies

By means of modern design-based stereology, we have shown structural adaptations of SG neurons to low-intensity treadmill training, i.e., remarkable neuron hypertrophy. From the novel stereological data raised here, further investigations are needed to shed light on the mechanistic aspect of neuron hypertrophy. What role does neuron hypertrophy play? Could neuron hypertrophy be assigned to the functional overload induced by physical exercise?

ACKNOWLEDGMENTS

We thank Wanderley Lima Guidi for technical assistance. We also thank Prof. Terry M. Mayhew (University of Nottingham, UK) for advice on sampling and stereological estimation. The authors are grateful to the reviewers for their constructive and positive comments, which improved the article.

REFERENCES

Abraham P, Picquet J, Bickert S, Papon X, Jousset Y, Saumet JL, Enon B. 2001. Infra-stellate upper thoracic sympathectomy results in a relative bradycardia during exercise, irrespective of the operated side. Eur J Cardiothorac Surg 20:1095–1100.

Amaral SL, Zorn TM, Michelini LC. 2000. Exercise training normalizes wall-to-lumen ratio of the gracilis muscle arterioles and reduces pressure in spontaneously hypertensive rats. J Hypertens 18:1563–1572.

American College of Sports Medicine. 2006. Guidelines for exercise testing and prescription. Philadelphia, PA: Lippincott, Williams and Wilkins.

Bozner A, Meessen H. 1969. The ultrastructure of the myocardium of the rat after single and repeated swim exercises. Virchows Arch B Cell Pathol 3:248–269.

Braendgaard H, Gundersen HJG. 1986. The impact of recent stereological advances on quantitative studies of the nervous system. J Neurosci Meth 18:39–78.

Brum PC, Da Silva GJJ, Moreira ED, Ida F, Negrão CE, Krieger EM. 2000. Exercise training increases baroreceptor gain sensitivity in normal and hypertensive rats. Hypertension 36:1018–1022.

Brüel A, Nyengaard JR. 2005. Design-based stereological estimation of the total number of cardiac myocytes in histological sections. Basic Res Cardiol 100:311–319.

Cabello CR, Thune JJ, Pakkenberg H, Pakkenberg B. 2002. Ageing of substantia nigra in humans: cell loss may be compensated by hypertrophy. Neuropathol Appl Neurobiol 28:283–291.

Chester M, Hammond C, Leach A. 2000. Long-term benefits of stellate ganglion block in severe chronic refractory angina. Pain 87:103–105.

Cornelissen VA, Fagard RH. 2005. Effects of endurance training on blood pressure, blood pressure–regulating mechanisms, and cardiovascularrisk factors. Hypertension 45:667–675.

Cox KL. 2006. Exercise and blood pressure: applying finding from the laboratory to the community setting. Clin Exp Pharmacol Physiol 33:868–871.

De Angelis KLD, Oliveira AR, Ago PD, Peixoto LRA, Gadonski G, Lancchini S, Fernandes TG, Irigoyen MC. 2000. Effects of exercise training on autonomic and myocardial dysfunction in streptozotocin-diabetic rats. Braz J Med Biol Res 33:635–641.

Eisele JC, Schaefer I, Nyengaard JR, Post H, Liebetanz D, Brüel A, Mühlfeld C. 2008. Effect of voluntary exercise on number and volume of cardiomyocytes and their mitochondria in the mouse left ventricle. Basic Res Cardiol 103:12–21.

Foster GL. 1956. The effects of exercise on respiratory exchange and peripheral blood flow. Med Arts Sci 10:145–151.

Foster GL, Reeves TJ. 1964. Hemodynamic responses to exercise in clinically normal middle-aged men and in those with angina pectoris. J Clin Invest 43:1758–1768.

Freeman JV, Dewey FE, Hadley DM, Myers J, Froelicher VF. 2006. Autonomic nervous system interaction with the cardiovascular system during exercise. Progr Cardiovasc Dis 48:342–362.

Gardner MJ, Kimber S, Johnstone DE, Shukla RC, Horacek BM, Forbes C, Armour JA. 1993. The effects of unilateral stellate ganglion blockade on human cardiac function during rest and exercise. J Cardiovasc Electrophysiol 4:2–8.

Gundersen HJG. 1977. Notes of the estimation of the numerical density of arbitrary profiles: the edge effect. J Microsc 111:219–223.

Gundersen HJG. 1986. Stereology of arbitrary particles. A review of unbiased number and size estimators and presentation of some new ones, in memory of William R. Thompson. J Microsc 143:3–45.

Gundersen HJG. 1988. The nucleator. J Microsc 151:3–21.

Gundersen HJG, Jensen EB, Kiau K, Nielsen J. 1999. The efficiency of systematic sampling in stereology: reconsidered. J Microsc 193:199–211.

Jones WB, Foster GL. 1964. Determinants of duration of left ventricular ejection in normal young men. J Appl Physiol 19:279–283.

Kokkinos PF, Papademetriou V. 2000. Exercise and hypertension. Coron Artery Dis 11:99–109.

Krout KE, Mettenleiter TC, Loewy AD. 2003. Single CNS neurons link both central motor and cardiosympathetic systems: a double-virus tracing study. Neuroscience 118:853–866.

Lima AR, Nyengaard JRN, Jorge AAL, Balieiro JCC, Peixoto C, Fioretto ET, Ambrósio CE, Miglino MA, Zatz M, Ribeiro AACM. 2007. Muscular dystrophy-related quantitative and chemical changes in adenohypophysis GH-cells in golden retrievers. Growth Horm IGF Res 17:480–491.

Mayhew TM. 2008. Taking tissue samples from the placenta: an illustration of principles and strategies. Placenta 29:1–14.

Mayhew TM, Gundersen HJG. 1996. ''If you assume, you can make an ass out of u and me'': a decade of the disector for stereological counting of particles in 3D space. J Anat 188:1–15.

Minitab (version 15). 2007. Minitab reference manual. Minitab Inc. State College PA, USA.

Mohan RM, Choate JK, Golding S, Herring N, Casadei B, Paterson DJ. 2000. Peripheral pre-synaptic pathway reduces the heart rate response to sympathetic activation following exercise training: role of NO. Cardiovasc Res 47:90–98.

Mueller PJ. 2007. Exercise training and sympathetic nervous system activity: evidence for physical activity dependent neural plasticity. Clin Exp Pharmacol Physiol 34:377–384.

Negrão CE, Moreira ED, Santos MCLM, Farah VMA, Krieger EM. 1992. Vagal function impairment after exercise training. J Appl Physiol 72:1749–1753.

Nieto JL, Lavianda ID, Guillen A, Haro A. 1996. Adenylyl cyclase system is affected differently by endurance physical training in heart and adipose tissue. Biochem Pharmacol 51:1321–1329.

Nyengaard JR. 1999. Stereologic methods and their application in kidney research. J Am Soc Nephrol 10:1100–1123.

Nyengaard JR, Gundersen HJG. 1992. The isector: a simple and direct method for generating isotropic, uniform, random sections from small specimens. J Microsc 165:427–431.

O'Sullivan SE, Bell C. 2000. The effects of exercise and training on human cardiovascular reflex control. J Auton Nerv Syst 81:16–24.

Peruzzi D, Hendley ED, Forehand CJ. 1991. Hypertrophy of stellate ganglion cells in hypertensive, but not hyperactive, rats. Am Physiol Soc 0363–6119:R979–R984.

Randall WC, Euler DE, Jacobs HK, Wehrmacher W, Kaye MP, Hageman GR. 1976. Autonomic neural control of cardiac rhythm: the role of autonomic imbalance in the genesis of cardiac dysrhythmia. Cardiology 61:20–36.

Ribeiro AACM. 2006. Size and number of binucleate and mononucleate superior cervical ganglion neurons in young capybaras. Anat Embryol (Berl) 211:607–617.

Ribeiro AACM, Davis C, Gabella G. 2004. Estimate of size and total number of neurons in superior cervical ganglion of rat, capybara and horse. Anat Embryol 208:367–380.

Silva GJ, Brum PC, Negrão CE, Krieger EM. 1997. Acute and chronic effects of exercise on baroreflexes in spontaneously hypertensive rats. Hypertension 30:714–719.

Skarda RT, Mur WW, Swanson CR, Hubbell JAE. 1986. Cervicothoracic (stellate) ganglion block in conscious horses. Am J Vet Res 47:21–26.

Somers VK, Conway J, Johnston J, Sleight P. 1991. Effects of endurance training and blood pressure in borderline hypertension. Lancet 337:1363–1368.

Sterio DC. 1984. The unbiased estimation of number and sizes of arbitrary particles unsing the disector. J Microsc 134:127–136.

Wallis D, Watson AHD, Mo N. 1996. Cardiac neurones of autonomic ganglia. Microsc Res Tech 35:69–79.